



A Review on High-Velocity Oxy-Fuel (HVOF) Coating Technique

Kalluri Anusha¹ · Bharat Chandra Routara² ·
Spandan Guha²

Received: 30 August 2022 / Accepted: 28 November 2022 / Published online: 2 January 2023
© The Institution of Engineers (India) 2023

Abstract Thermal spraying is a technique for applying coatings with thicknesses ranging from 10 μm to a few mm over mechanical components to improvise distinct and particular functional features, such as resistance to wear and corrosion, compatibility with human health and safety, as well as a wide range of friction coefficients, and so forth. An average particle viscous enthalpic jet may be created with a particle size range of 0.01 μm to some μm . Among different thermal coating processes, high-velocity oxy-fuel coating is new in this family and one of the most rapidly used coating techniques and this technique can provide a heavily dense coating with a porosity level of $< 1\%$. Moreover, HVOF coating possesses considerable adhesion and hardness value and can extend the life of coated equipment by improving wear, erosion and corrosion resistance properties. The used particles in this process carry higher potential energy and that ultimately helps to form a high-quality coating. With careful control over the cooling rate, this coating technique can deposit coating with thickness up to 1.5 mm to reduce residual stress.

Keywords Coating · Thermal spraying · HVOF · Review article

Introduction

The thermal spraying technique is one of the type of coating processes in which material in molten or heated state is sprayed over the work piece surface [1–3]. In this process, coating materials generally are metals, alloys, plastics, ceramics, etc., melted or heated by electrical (plasma or arc) or chemical (combustion flame) source. This type of coating techniques can provide coating on a large area with higher coating thickness compared to other deposition techniques (e.g. chemical vapour deposition (CVD), physical vapour deposition (PVD) and electroplating etc.). Coating materials generally used for this process are fed in the form of powder or wire in a molten or semi-molten state. These materials are then accelerated towards the substrate surface in the form of micrometre size particles. Among the several varieties of thermal spraying techniques, HVOF coating is one of the most prominent ones [4, 5]. The HVOF coating technique utilizes the combustion of hydrogen and natural gases or liquid fuel like kerosene and then particles of fuel along with oxygen particles mixed and atomizes within the combustion area under the condition that monitors the correct combustion mode and pressure. Within the combustion chamber of the HVOF system, oxygen combusts with gaseous or liquid fuel to produce high kinetic energy under the controlled heat input. The coating materials are now introduced into the chamber and heated by the hot gas stream up to a molten or semi-molten state. After this, high-velocity gas stream propels the coating material particles near supersonic speed before impact on to the substrate's surface [6–8]. The flame with the powder accelerated up to supersonic velocity due to its passing through the converging–diverging nozzle. Powder particles are fallen on the surface of the substrate with a very high velocity, which results in very high-quality coating (e.g. highly dense, 0.5–2% porosity, etc.) [4–8]. The

✉ Spandan Guha
spandan.guha@yahoo.com

¹ Department of Mechanical Engineering, Raghu Institute of Technology, Visakhapatnam, Andhra Pradesh 531162, India

² School of Mechanical Engineering, Kalinga Institute of Industrial Technology, Bhubaneswar 751024, India

developed film is also less oxidized due to particles spending less time within the heat source as its speed is the very high and lower flame temperature (around 3000 °C) compared to other processes. So all together high particle velocity, low dwell time and uniform heating produce HVOF coating a very tightly bonded and dense coating process. Coating chemistries are very predictable, and coatings have fine, homogeneous microstructures. Coatings produced by the HVOF system have some outstanding properties. The HVOF coating has less than 2% porosity, and even some of the coating has 0.5% of porosity. Carbide coating sprayed with a HVOF system can exhibit bond strength up to 69 MPa. This is significantly higher than other coatings materials and coating processes. Micro-hardness: a typical micro-hardness within the range of 1100–1350 Diamond Pyramid Hardness (DPH) 300 can be achievable with the help of 12% Tungsten Carbide/Cobalt coating [5–7]. Factors like short dwell time and lower temperature of HVOF produce significant wear and impact-resistant coating. The HVOF produces higher coating thickness than combustion, plasma or wire coatings of the same materials. Because of the higher thickness, the stress relieving 'short peeing' effect due to high-velocity particles is withstanding. Some of the Tungsten Carbide (WC) coatings can achieve a thickness higher than 6.4 mm [1,3,4–7]. Significant compressive residual stress and very low tensile stresses enhance the fatigue life of coated components at the same time while reducing the chances of cracking and permitting greater coating thickness. By choosing proper combination of process parameters and selecting suitable materials, this process can impart significant amount of wear, fretting, erosion and cavitation resistance properties [3–5]. The properties like higher density and bond strength make HVOF to create self-protection ability against acidic and alkaline solution. Additionally, due to have some significant metallurgical properties HVOF coating can generate resistance against oxidation and corrosion. Superiority in the surface finish makes HVOF coatings materials

enable to use for different purposes. Even coatings can be machined, ground, lapped or honed to improve their surface finish [6–10]. Mainly there are two types of HVOF coatings, e.g. liquid and gas, and a comparison table is presented in Table 1.

Brief Historical Viewpoint

The evolution of the thermal spraying technique took place around 1900s when Dr. Max Ulrich Scoop of Zurich realized that coating can be developed with the help of a stream of molten particles impinging upon it. This is the time when engineers used to break the fine particles into super-fine particles or powders with the help of high-pressure gas. Dr. Schoop's evolution ultimately helped to develop the thermal spraying technique [8, 9]. Then in the year 1910 Dr. Schoop along with some of his German associates developed one composed of equipment by which coating can be made from molten and powder metallic. In the year of 1912, Dr. Schoop and his associates used the metalizing principle to develop one instrument for spraying wire from solid metal [8, 10, 11]. Nowadays, metalizing principle is known as oxy-fuel or flame spraying. At present, a wide range of oxy-fuel techniques are available, e.g. ceramic powder, metallic powder, ceramic rod, HVOF etc. Different thermal spraying techniques are highlighted below [11]. The schematic diagram of thermal spray coating is shown in Fig. 1.

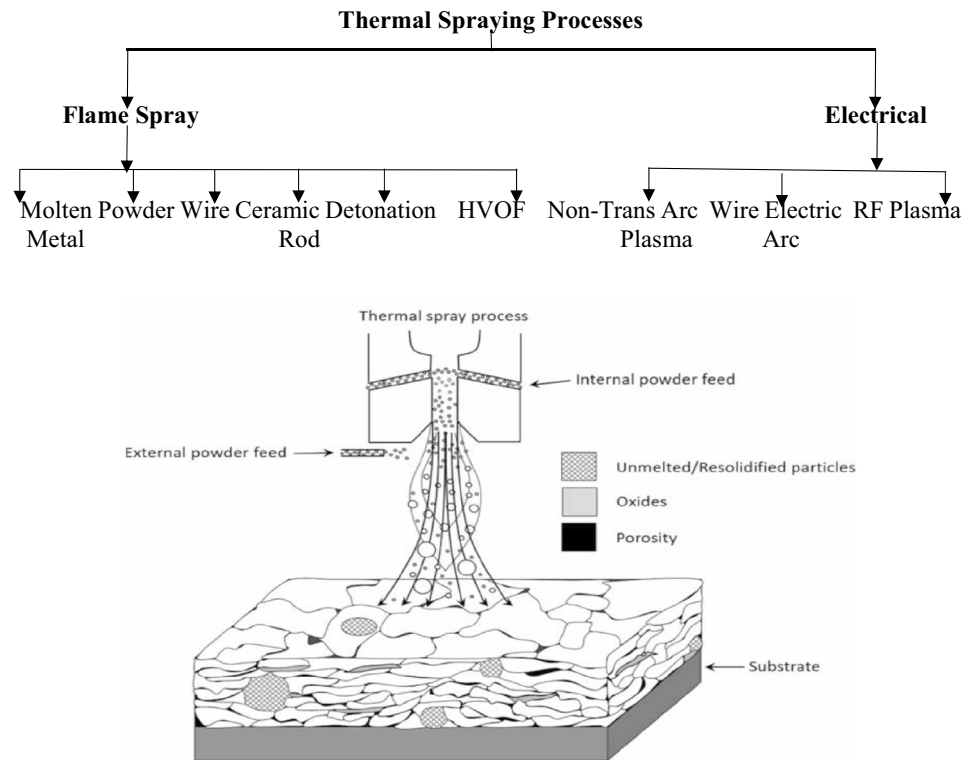
Spray Guns and Coating Parameters

The typical operating pressure is in the range of 0.3–0.6 MPa. Oxygen serves as the oxidizing gas and fuels such as hydrogen, propylene, propane, methane and acetylene may achieve nozzle exit velocities of up to 1600 m/s. Shock diamonds and oblique shock waves can be generated

Table 1 Comparison between gas fuel and liquid fuel HVOF technology

Components	Gas fuel HVOF	Liquid fuel HVOF
<i>General characteristics</i>		
Fuel options	H ₂ , CH ₄ , C ₂ H ₄ , C ₃ H ₆ , C ₃ H ₈	Kerosene
Combustion pressure	0.55 MPa (80 PSI)	0.55–0.83 MPa (80–120 PSI)
Gas velocity	1800–2100 m/s	2000–2200 m/s
Particle velocity	450–600 m/s	475–700 m/s
Powder injection	Axial feed (Hotter zone)	Radial feed (Cooler zone)
Powder injection pressure	Higher	Lower
Spray rate	Up to 120 g/min	Up to 200 g/min
<i>Consumption comparison (per hour of operation)</i>		
Fuel	43,800 L H ₂ or 5280 L C ₃ H ₆ , C ₃ H ₈	28 Litters Kerosene
Oxygen	18,420 L	61,400 L
Water	600 L	2375 L

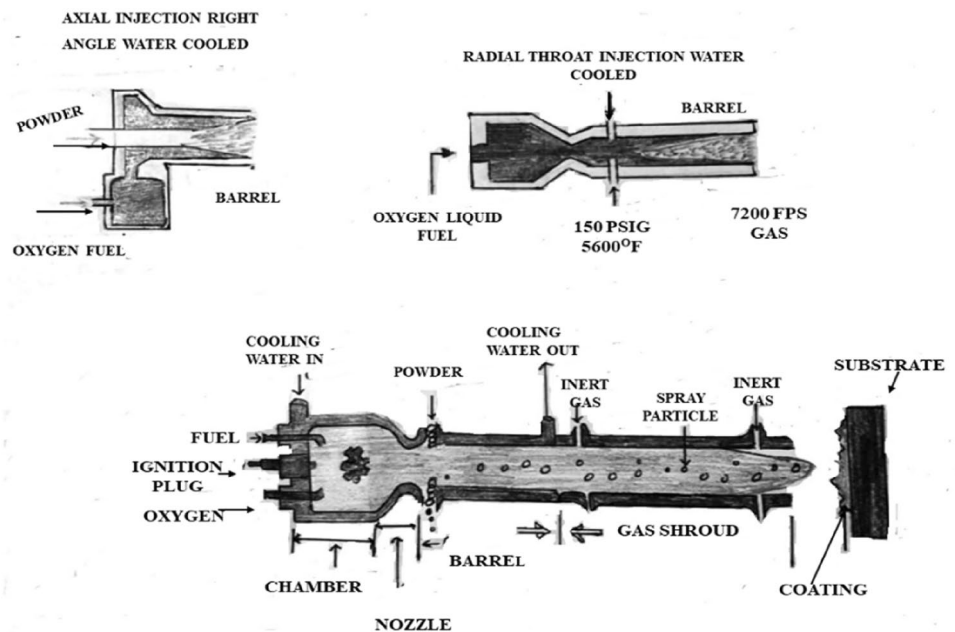
Fig. 1 Thermal spray coating process [11]



by this flow. The jet is under-expanded since the flow is supersonic and the pressure is above atmospheric, as it has the barrel, pressure is reduced below atmospheric, and temperature decreases at a faster rate because of the increased velocity [12]. The water-cooled HVOF concept has evolved into the axial flow device depicted in Fig. 2b. Figure 2c depicts the last stage of development [13]. There

are two ways in which powder is injected: either via throat of the barrel or through its diverging part. Low pressure is caused by an under-expansion situation downstream of the neck. Consequently, powders can be injected at this point to facilitate injection and containment and multiple-port powder injection is conceivable for more uniform loading of the exit stream and effective utilisation of the available

Fig. 2 Design changes that are typical with HVOF: **a** the “Jet Kote principle”, **b** the combustion chamber and axial injection, and **c** the axial powder injection chamber with radial chamber



heat. As a rule, operational data show that radial injection can produce spray rates at least twice as high as axial injection per unit of energy. This design has also allowed for a rise in combustion gas pressure [14].

By using liquid petroleum instead of flammable gas and air in place of oxygen, J. W. Browning developed the high-velocity air fuel (HVAF) method [11]. Speeds up to 2000 m/s may be reached even at lower temperatures because of the high pressure in the chamber of combustion (above 0.8 MPa) and the amount of air (about 8–10 m³). Air cooling is another option for the gun. It was not long ago when kerosene was used as an alternative to flammable gases and oxygen was used in its place of air, which enabled extraordinarily high dissipated powers to be achieved (almost 300 kW). Components of the gun are subjected to high temperatures and oxidation, which need a precise water cooling design for the combustion chamber and nozzle [11,13–15].

Flow modelling has been the subject of several studies. The transition is from basic isentropic one-dimensional flow to three-dimensional supersonic flow [15–18]. In such hot flows, it is clear that it is important to figure out the temperature and speed of the particles. As a result of this, traditional equations, numerically influence the drag force on the particle [16–20]. For supersonic speeds, the coefficient of drag is recalculated. The MCrAlY particles smaller than 25 µm in MCrAlY are largely affected by shock diamonds and bow shocks produced near the substrate [19]. Spray guns (Fig. 2b) used in this study produces stainless steel particles (mean diameter 28 µm) at almost same velocity regardless of injector position and this velocity increases linearly as the pressure within the chamber increases (0.5–0.95 MPa). As a result, the range of temperatures lies within the range of 1610–1750 K. But the position of the radial injector (Fig. 2c), which can be changed from upstream to downstream of the nozzle, has a huge effect on the temperature. For particles between 1700 and 1800 K, the oxygen concentration in the coating ranges from 0.25 to 0.8%, depending on the particle temperature. Oxidation occurs in the jet core [13] in the area of mixing air with the jet and finally in the production of oxidation products.

In a high-pressure chamber, it is the deflagration of a hydrocarbon molecule (C_xH_y) with either oxygen or air as the oxidizer at a pressure between 0.24 and 0.82 MPa. When taking into consideration the local pressure and temperature, the nozzle is capable of producing gas velocities up to 2000 m/s [13]. The reaction energy or enthalpy, in highly compressed explosive medium (about 2 MPa), sent out a shock wave that moved the hot particles [16]. Gas velocities above 2000 m/s are not uncommon. Instead of being fed continuously into the gun as in the previous two

devices, this device cycles through flammable gases and powders at a frequency of 3–8 Hz [13, 15, 19, 20].

Geometrical Constraint

Regardless of the spraying method employed, it's a line of sight approach. Only those areas that can be reached by the particle stream are coated. The spray pattern on the component can be reduced up to 200 µm in size using rotating masks, but more work needs to be done. The smallest diameter that can be covered sensibly during external spraying is approximately 1 mm [19]. When it comes to internal thermal spraying, the diameter of the cylinder that may be sprayed is around 30 mm. The height-to-diameter ratio is the limiting element in cavities (i.e. blind holes). A diameter of 8 mm is required for a ratio of around 1 [20]. Thermal spray guns are equipment used to feed, accelerate, heat and direct the spray pattern's material flow. According to the method of energy production, they can be divided into three distinct groups [21].

Spray Material

Powders, wires, rods, and cords can be put into the enthalpic jet to change the speed and temperature distribution of the particles to match the materials being sprayed and the qualities of the coatings that are wanted. The size distribution (d_{10} – d_{90}) must match the spray gun melting capabilities (d_{50}) of the material (mass enthalpy of the emitting jet and interaction time) [18]. The powder feeder device must also be able to handle the flow of the powder (several technologies exist). It is important to keep the feedstock moisture content and particle size distribution as low as possible before spraying to maximize flow ability. A minimum of 24 min at temperatures ranging from 60 to 80 °C must be used to remove the moisture in the feedstock. When using agglomerated composite materials, the distribution of each particle's components must be as consistent as feasible [20]. The powdered feedstock is commonly accelerated, heated and liquefied using spray gases. The usage of ductile materials is implied by the use of wire. Cored wires can be made from non-ductile materials as well as ductile ones. Powdered metals or ceramics that don't bend easily are surrounded by a coating of a material that does. Ceramics are the primary use for rods and cords [15,17–19]. The molten material is atomized and moved by auxiliary gas that is pumped into the spray gun. At the same time, the wires, rods, and cords are constantly moved forward at a speed that lets the jet that comes out of the spray gun under investigation melt the ends of the wires, rods, and cords [22].

The d_{10} and d_{90} dia. (i.e. 10 percent volume of elements below d_{10} and 10 percent vol. percent of particles above d_{90}) and the average diameter of the particle size distribution, d_{50} , are used to describe powders (e.g. 22–45 μm). Spools of ductile-material wires are offered for purchase. In terms of diameter, they measure between 1.20 and 4.76 mm. It is more difficult to feed larger, stiffer wires ($d > 2$ mm) due to the increased effort and strain required to uncoil them. There are a few millisecond spray times for ceramic rods with diameters of 3.16, 4.75, 6.35 and 7.94 mm [17, 21]. Cords are made by encasing ceramic particles in cellulose or polyester. In the processing of ceramic particles, either an organic binder is used, which begins to degrade at around 250 °C and decomposes completely at around 400 °C or a mineral glue like “bohemite ($\text{Al}(\text{OH})_3$)”, which binds the ceramic particles together near their melting point temperatures. Cords provided on spools have a 100 m length, allowing for several hours of spraying, compared to rods. Between 3.16 and 6.35 mm in diameter, they are the most common [15, 16, 21].

Coating Adhesion

Figure 3 depicts the fundamental design of the HVOF spray system using the diamond Jet gun as an illustration [22]. HVOF process possesses higher bond strength, less porosity compared to other thermal spray processes (e.g. plasma spraying, flame spraying, and electric arc spray etc.) as high velocity of particles creates more impact over the substrate surface [23–26]. Particle velocity, flame temperature, and spray atmosphere are the primary distinctions between spraying techniques. The coating procedure typically affects coating properties such as porosity, bond strength, and oxide content. Table 1 demonstrates the characteristics of tungsten carbide-cobalt (WC-Co) coatings sprayed using various

Fig. 3 Schematic cross section of HVOF gun [28]

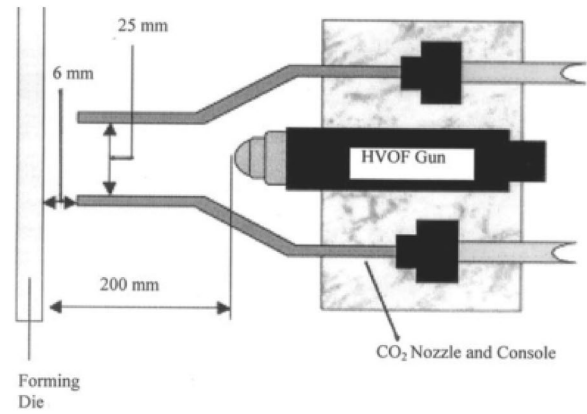
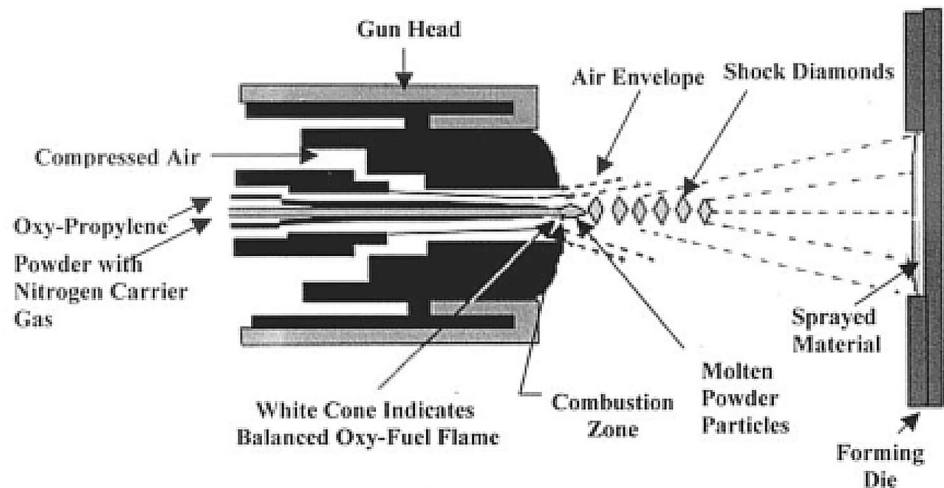


Fig. 4 Schematic of carbon dioxide nozzle layout and distances used [28]

techniques [27]. Figure 4 is a layout and distance diagram of a carbon dioxide nozzle.

As shown in the literature [29] a copper base, 25 s after the spray method began (Helium, 2 MPa 300 K), immediately before the formation of the coating on the copper surface [30]. Particle concentration and velocity in the flow have a direct impact on the induction time. Plastic deformation occurs when the particle is subjected to a tension larger than its yield stress due to a collision with sufficient energy. In the area of the contact zone, high plastic strain rates are seen upon impact, leading to adiabatic heating and localized material softening. It causes shear instabilities, which are responsible for the ejection of particle–substrate interface solid-state jets of material [28, 31]. Allowing for direct metal-to-metal contact, the oxide layer has been partially eliminated. Low-velocity particles abrade the substrate, whereas high-velocity particles deposit and create a coating on the surface. This is shown schematically in Fig. 5 [32].

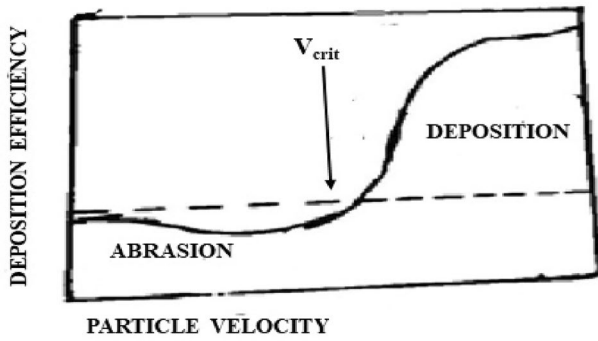


Fig. 5 Particle velocity and deposition efficiency are shown to be correlated in the following diagram. The critical velocity, V_c , is defined by the transition between abrasion and deposition at low velocities

Adhesion and elastic deformation energy created by particle impact may be compared using an easy-to-understand model devised by B. R. Marple [33]. At first coating layer is formed when the adhesion energy exceeds the elastic deformation energy, and this has been researched.

Fig. 6 Various spray material critical velocities were experimentally determined. The error bar takes into consideration the wide range of powder purities that are accessible

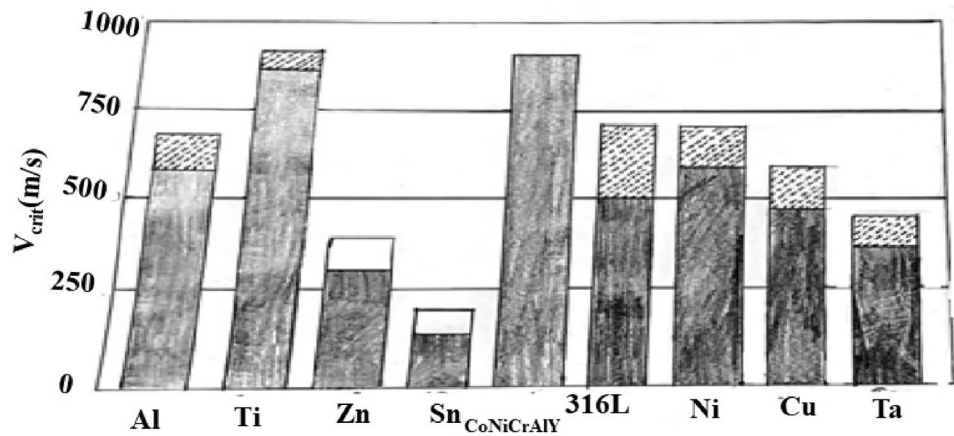
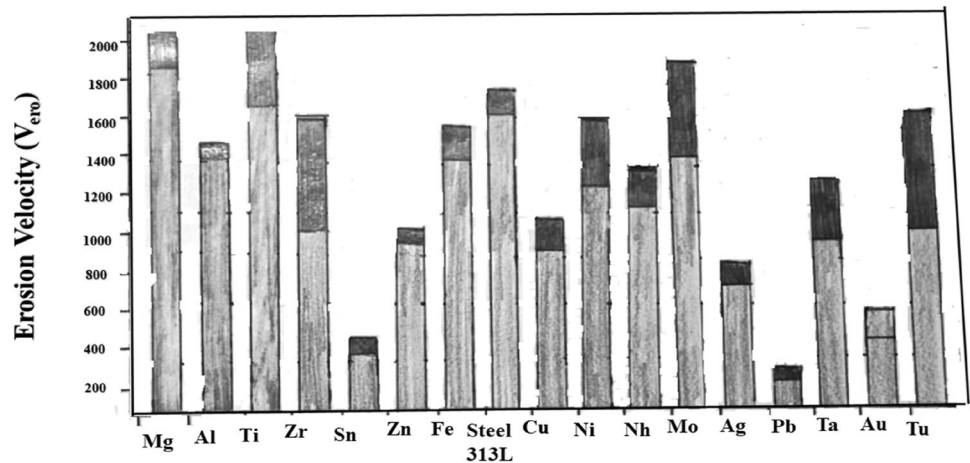


Fig. 7 The erosive velocity of different metals was calculated for 25 m particles



It has been discovered that the best spraying circumstances are dependent on the qualities of sprayed materials and surfaces as well as spray particle sizes and temperatures [28]. Various spray materials and substrates have had their critical velocities calculated. Gartner and colleagues [34] looked at the critical velocities of several spray materials on a copper substrate. Figure 6 sums up the findings.

A study by Gartner et al. [32] found that particle’s particular mass and temperature affect their critical velocities. The hitting particle will cause significant erosion if its velocity exceeds the range of hydrodynamic penetration. The erosion velocity ($V_{erosion}$) was calculated by Schmidt et al. [35, 36]. It is faster than the device’s critical speed observed (Fig. 7).

Spray Specifications

When adhering a coating to the surface and forming the following layer, the most important impact factors are particle velocities and materials, together with the substrate’s material qualities. Gas stagnation pressure, temperature,

molecular weight, and particle shape and size all affect particle velocity [37, 38].

When injecting particles axially with a DJ-2700 gun, using a JP-5000 gun and injecting radially increases the oxygen content of the coating only slightly (316L). As a result, while using JP-5000, where the particles are at a lower temperature (about 800 K lower), O₂ in the flame cools them even further, lowering their oxidation content even further. A gas shroud attachment for commercial HVOFs has been developed by Ishikawa et al. [14] to minimize oxidation using a shroud gas, although at a considerably lower flow rate. WC–Co particle velocities rise from 760 to 850 m/s with the gas shroud arrangement, but particle temperatures fall from 1950 to 1830 °C due to a decreasing flame at a pressure of 0.72 MPa. The density rose, decomposition of WC was 6 to 2.5%, and corrosion resistance and good wear resistance greater than without a shroud were also achieved. High-density coatings with little oxidation and no carbide breakdown can be achieved by raising the particle velocity while reducing the temperature of the powders used in HVOF or HVAF. Because of this, Kawahita et al. [37] modified the pistol by including a mixing chamber between the combustion chamber and the nozzle. Nitrogen is added to the combustion gas in the combustion chamber to its lesser temperature. Operating parameters for the altered JP-5000 include kerosene consumption of 0.29–0.35 l/min, N₂ consumption of 0.5–2 Nm³/m, and O₂ consumption of 0.55–0.73 Nm³/m. Thus, titanium (Ti) coatings with a high density that are resistant to corrosion were developed [38].

When it comes to HVOF gun development, researchers have concentrated on reducing particle temperature and boosting their velocity for more than two decades already. Up to 1 MPa chamber pressure can produce spray particle speeds of up to 650 m/s [39]. Hydrogen pilot flame (88 Litres/min, air 500 L/min) ignites combustion chamber fire when power rises up to 300 Kilo Watt (Kerosene 31 l/h, O₂ 965 l/min). For example, Trompeter et al. [40] used an HVAF gun to spray NiCr powder (melting point T_m = 1400 °C), which resulted in a particle velocity of 670 m/s. In comparison with hardness of NiCr, spraying soft surfaces produced mostly deeply penetrated solid splats, whereas spraying hard substrates resulted in more heavily molten splats. They hypothesized that the quantity of plastic deformation owing to substrate hardness would explain this occurrence by converting particle kinetic energy into heat. Peening and persistent compressive stresses in coatings are the second results of high-velocity impacts [32, 41, 42]. Studies show that HVOF coatings have minimal surface residual stress and typically have tensile stress, but the stress within thin films is substantial and mostly in compression, according to the measurements. Pumping on a stainless steel substrate results in a 100-m-long hardening zone, which is why this peening effect is so important for metals like stainless steel.

The HVOF technique creates coatings with a high density because of the particles with high kinetic energy (400–650 m/s) [37] (porosity less than 3%). As a result, materials like WC may be deposited at temperatures below their melting point, minimizing oxidation and degradation. It is now possible to use spray guns to apply materials that lack the extraordinary copper's ductility or aluminium and they are more vulnerable to oxidation, than Ti [40].

Influence of HVOF Process Parameters

The qualities of the coating, resistance to corrosion and erosion, and other factors are often improved by optimising the spraying parameters. The distance of spray, powder feed rate, oxygen flow rate, fuel flow rate and carrier gas used are few factors that affect coating qualities. Brezinová et al. [43] examined the impact of milling time (36 h) on the mechanical properties of SAE 1020 steel that had been sprayed with HVOF and coated with WC/Co and WC/Co-CNT. The findings demonstrated that the inclusion of Carbon Nano Tube (CNT) enhanced the coating's mechanical properties, including hardness, fracture toughness, and apparent yield stress. The effects of heat treatment (using oxyacetylene flame) on the adhesion resistance, microstructure, micro-hardness and erosive wear of HVOF-sprayed NiCrBSiW coated plain carbon steel were studied by Rodriguez et al. [44]. After the post-spray heat treatment, the coating's porosity was reduced. Additionally, better metallurgical bonding was created after the post-spray heat treatment, which improved the coating's cohesion and adhesion strength. Using a factorial experimental approach, Gil et al. [45] investigated the effects of process factors on the adhesion strength and microstructure of NiWCrBSi coatings formed by HVOF process. The coating's adhesion strength and porosity are most significantly impacted by the spray distance and equivalency ratio. Table 2 makes it evident that Cr₂O₃-4%CNT, NiCrBSi, Cr₃C₂-NiCr and Ni-20Cr coatings are sprayed with HVOF and deposited under ideal conditions offer higher mechanical properties.

Effect of Residual Stresses in HVOF Coatings

The process of thermal spray coating encompasses a broad variety of other processes, some of which include wire-arc, HVOF, plasma spraying, and many others that are utilised in a variety of various applications. One of the most important things to think about when it comes to coating performance is how the stresses left over from the coating process affect the life and behaviour of the coating layer [56]. It could be very important to the evaluation process to measure these stresses. Because of this, a lot of research has been done on

Table 2 Process parameters of HVOF-sprayed coatings [46–55]

Sl. No	Substrate	Coating material	Particle size (μm)	Oxygen rate of flow (L/min)	Fuel (propane/LPG) flow rate (L/min)	Air flow rate (L/min)	SOD (mm)	Powder feed rate (g/min)
1 [46]	SA 516	Ni–20 Cr 81% Ni Ni–20Cr 73% Ni Ni–20Cr 65% Ni	13.9 12.0 10.99	262	63	610	151	34–40
2 [47]	T_91	Cr_3C_2 –26%Ni Cr	14–46	262	64	640	20	60
3 [48]	Alloy 80A	Cr_3C_2 –26Ni Cr NiCrMoNb	44/16 53/20	845 840	20	–	365 365	35 40
4 [49]	P-91	Stellite-6 Cr_3C_2 –25%NiCr Hastelloy C-276	– –45 to +15 –52 to 20	995 872 857	0.460 0.453 0.685	–	360 380 380	–
5 [50]	T-22	Cr_{203} Cr_{203} -1%CNT Cr_{203} -4%CNT	44 to 11	254	83	600	200	20
6 [51]	AISI 316 Stainless steel	Ferrous type amorphous powder	–55 to +16	250 249 260	65 64 66		233 2340 234	34 40 37
7 [52]	T_91	76 Cr_3C_2 –24 Ni Cr	–44 to +16	249	61	610	180	–
8 [53]	T-22 MDN 310 SF 800H	WC_ Cr C–Ni	17 to 43	249	66–70	549	178	23
9 [54]	T-22 SF 800H MDN 310	Cr_3C_2 –34% Ni Cr + 6% Si	–46 + 14	250	64–69	549	178	38
10 [55]	T_91	66% Cr_3C_2 –34% (Ni–20 Cr) 75% Cr_3C_2 –25% (Ni–20Cr) 80% Cr_3C_2 –20% (Ni–20Cr) 90% Cr_3C_2 –10% (Ni–20Cr)	–	251	61	910	200	28

how to measure and calculate the quantitative and qualitative residual stresses. During the coating process, most of the work was done using pure experimental methods to measure the residual stresses. Others get the stress values using a method that is a mix of experiments and math [57].

Sources of Residual Stresses

Residual stresses in coatings that are sprayed with heat come from two main places. The first is the sudden temperature decrease from the melting point to the substrate temperature experienced by the sprayed particles. This kind of stress is called intrinsic, quenching, or deposition, and it is tensile. The second source, which may be the most important, is that the coating and the substrate have different coefficients of thermal expansion (CTE). This happens when the average temperature of the coating system after the deposition process starts to drop towards room temperature. This is called secondary cooling [57]. Then, the difference in how much the substrate and the coating shrink when heated leads to

the residual stresses. Aside from the two main causes, there may be other things that indirectly cause residual stress. For example, the amount of residual stress left after deposition depends on how fast the coating particles are moving. This has to do with the speed of the coating and the size of the particles.

Literature shows that in HVOF coating systems, residual stresses come from [56, 57]

1. The process of coating deposition. When particles hit something, they freeze and shrink, which creates tensile stresses that are mostly relieved by the formation of tiny cracks in the coating.
2. Stress from the wrong materials. When the parts that have been coated cool down to room temperature.
3. Differences in the thermal expansion coefficients of the coating and the material underneath it.

Parameters Affecting Residual Stresses

The generation of residual stresses is influenced by a number of process variables, including deposition speed, spray gun velocity, coating temperature, coating thickness, etc. However, these parameters cannot be improved purely based on residual stresses; it is also necessary to take the final coating's quality into account.

Following is a broad breakdown of the processes in the coating process that have an impact on coating quality [58]:

- Spray particle movement →
- particle collision and deformation →
- coating formation →
- splat interactions →
- pore formation →
- coating build-up → and final coating layer.

Importance of Residual Stresses Calculation

In general, compressive residual stresses are preferable, and unless they are present in relatively high quantities, their existence usually has no negative effects on the coating system. Tensile residual stresses are typically more detrimental and cause numerous coating issues, including fatigue failure and the initiation and spread of cracks, which can result in interface delamination. Drilling holes is one of the most popular methods for evaluating residual stresses [59, 60]. Typically, drilling in this procedure is done subtly at the micro-level until the substrate is reached [57, 61, 62]. It is reasonable to infer that this procedure produces minimal stresses because it uses moderate feed rates, high cutting rates, and low drilling depths for each phase. A cooling time is also used in between every other drilling increment to ensure that there are no thermally induced stresses brought on by the drilling operation [62].

HVOF Wire Spraying

Due to the low impact velocities for the particles, wire flame spraying produces very porous coatings (over 10%). The high rate of wire flame spraying (up to 10 kg/h) makes it a major issue in terms of process economics, which is often the case. The automotive industry has been studying the HVOF wire spraying technique since 1995. There has also been spraying of molybdenum. Compared to plasma spray coatings, wire flame-sprayed thin films have lower friction resistance but are tougher and more wear-resistant [63]. Methane and oxygen were also sprayed on low-carbon steel. [64] Such thin films are also applied to nickel–chromium wires [65] and nickel–chromium alloys such as Cr₃C₂-NiCr [66]. Those treated guns with a fuel-oxygen had a strong resistance to heat corrosion, notably Ni-20Cr, with less than one percent porosity. As a last note, an HVOF/plasma jet gun and arc spray hybrid method [67] has been devised Table (3).

Mechanical Properties of HVOF Coating

Tribological Properties of HVOF Coating

The average coefficient of friction and volume lost by the coatings against various counter bodies are summarised in Table 4 [74]. It's interesting to note that while sliding against the identical counterpart, HVOF coatings had a lower coefficient of friction than other types of coatings. In comparison with other counter bodies, the volume lost by both coverings because of the Al₂O₃ ball is significantly higher. In comparison with Si₃N₄ and steel balls, the volume lost by coatings due to Al₂O₃ balls is precisely 2.7 and 20 times higher, respectively. Additionally, among the three counter bodies, the volume loss of the Al₂O₃ ball is the least. As a result, the Al₂O₃ ball was able to keep its initial curve throughout the test period. As a result, the Al₂O₃ ball has effectively pierced both coating surfaces [74].

Comparative Analysis in Between Different Coating Processes

Innovations in different coating processes, thermal spraying, CVD, PVD and other processes mainly rely over the evolution of their past developments. To deposit uniform thin film coating, many coating techniques are available in the market. Each techniques have their own pros and cons along with some important parameters. So utmost care should have been taken over key parameters during the process to get the desired coatings. In thermal spray process, by conveying gas stream, feed stock material will be heated, atomized and ultimately deposit over the prepared substrate surface [75].

As the materials are in heated state, they will transform into plastic or molten state, they become atomized and confined before accelerated towards the substrate's surface. Then the stroked particles over the substrate surface become flat and develop thin platelets. These flat particles then match up to the irregularities of the substrate surface. So it will provide considerable barrier protection over the surface. In PVD process, the developed exceptional properties in coating are due to the presence of highly ionized metallic vapours. In CVD process, it is possible to homogeneously coat 3D samples, whereas in physical vapour deposition PVD processes mainly have command over growth of coating. In Tables 2 and 3, comparison between different thermal spraying techniques and a comparison of HVOF with CVD and PVD have been highlighted [75–77] (Tables 5, 6, and 7).

Applications HVOF Process

Engineers use HVOF to coat technical components with cermet, metal, and some ceramic thin films that are generally 100–300 μm in thickness, enabling them to operate under harsh circumstances. Aside from wear resistance, they're being examined extensively for their higher corrosion and resistance to oxidation in comparison with different spraying methods. They are widely used in a variety of industries, including maritime, aviation, and automobiles. With their

help, a broad range of petrochemical system elements can be recovered.

Using HVOF, lower oxygen and fuel ratios allowed for the production of ultra-thin, pure aluminium films [105]. The HVOF process was used to spray iron-aluminide with 7–15% oxide [106]. With gaseous or liquid fuel, Ni-20wt% Cr spray creates less oxide, lower porosity, and lower melting evidence [107]. HVAF spraying on aluminium substrates results in a strong connection between the substrate and the Ni Cr particles, but there is no chemical bonding [108]. Waste-to-energy boilers use protective Ni Cr or Ni Cr Si B coatings to avoid corrosion [109]. To avoid corrosion, Ni Cr Mo Nb can also be used [110]. The HVOF coating made of super alloys can also be used as thermal barrier bonds [111, 112].

For HVOF and HVAF procedures, substantial research has been done on cermet from the start [113–119]. Spray cermet most typically employs WC-Co and $\text{Cr}_3\text{C}_2\text{NiCr}$.

Table 4 Tribological properties for different counter bodies in HVOF process

Counter body	Coating	average COF	Volume loss by ball (mm^3)	Volume loss by coating (mm^3)
Al_2O_3	HVOF	0.151	0.0269	1.4190
Si_3N_4	HVOF	0.135	0.0778	0.6631
AISI 52,100 Bearing ball	HVOF	0.148	0.1827	0.1317

Table 3 Mechanical properties of different coating materials and substrates [47,68–73]

Sl. No	Substrate	Coating material	Micro hardness (HV)	Porosity (%)	Surface roughness (μm)	Fracture toughness ($\text{MPa m}^{1/2}$)
1 [47]	ASME SA213 T-91	Cr_3C_2 -25%NiCr	755	2.5–3	5.36 ± 1.5	2.43 ± 0.9
2 [68]	1Cr18Ni9Ti	(a) 88WC-12Co	1181	0.99	4.49	4.57
		(b) 83WC-12Co	1120	0.84	2.47	4.64
		(c) Cobalt based alloy	553	–	–	2.58
3 [69]	Stainless steel (ss sus 400)	WC-12Co	1288.63	0.0721	6.55	–
4 [70]	AZ31 Magnesium alloy	WC	7.5 ± 4	3.7 ± 0.7	3.8 ± 0.3	3.6 ± 0.6
		CrC	74 ± 31	2.4 ± 0.5	2.9 ± 0.2	4 ± 1
5 [71]	SS-304	TiB_2 -50Ni	766.1	2.3	2–3	–
6 [72]	Ti6Al-4v	1. HVOF coating of conventional WC-Co	986 ± 111	2.6 ± 0.3	7.7 ± 0.4	4.2 ± 0.3
		2. HVOF coating of nanostructured WC-Co	1094 ± 105	1.5 ± 0.2	6.4 ± 0.1	5.6 ± 0.7
		3. HVOF coating of mixture of conventional WC-Co & CNT	1273 ± 150	2.8 ± 0.4	7.1 ± 0.5	4.7
		4. HVOF coating of nanostructured WC-Co & CNT	1396 ± 85	1.6 ± 0.3	6.6 ± 0.2	6.7 ± 0.2
7 [73]	En32	(a) WC-12Co	1250 ± 90	1.3	1.53	–
		(b) WC-10Co-4Cr	1140 ± 80	1.4	1.38	
		(c) Cr_3C_2 -25NiCr	830 ± 80	2.6	2.36	

Avoiding or at least reducing carbide breakdown as much as feasible is a vital part of coatings quality. Because of their corrosion and wear resistance (especially those containing NiCr), these coatings are commonly employed. A variety of other materials, like MoB and CoCr [120], which protect against erosion with liquefied Al–Zn alloy, a variety of Nickel–Titanium–Carbon (Ni–Ti–C) [121], which contains Ni-rich solution, Ni-rich spraying Ti-in addition to Ni-rich solution, and a variety of silicon nitride-based coatings [117] all of which are sprayed.

When it comes to coatings made using HVOF or HVAF technology, high temperatures are less of a rarity than fast speeds. Propylene devices may easily melt Ti [122]. High Weibull modulus values and thick and homogenous coatings, with rutile as the dominating phase, are achieved in contrast to previous spray processes. Chromium stabilizes the phase in most alumina [123]. Zirconia stabilized with yttria particles smaller than 10 m can be sprayed, and the production of adhesive and cohesive coatings may be influenced by sintering [124].

Without ceramic doping, nylon 11 is the most widely used polymer [125–127]. Degradation is usually limited to a change in colour due to the HVOF residence time being short enough (1 m/s). Abrasion and fatigue wear may be taken into account without doping powders in these coatings. Materials sprayed with a mixture of liquid fuel and oxygen are nearly identical to those sprayed with gaseous fuel. Higher velocities and lower temperatures are the primary distinctions.

When copper was heated to a temperature where it was highly deformable just below its melting point [128] extremely dense coatings could be produced. Coatings, on the other hand, were more durable than wrought iron [129].

Furthermore, the adhesion of Ni–Cr–9Cr–1Mo steel exceeded 70 MPa and had outstanding resistance to steam oxidation [127, 128]. With these HVOF process guns and a noble gas shroud, the thin film oxygen levels attained with vacuum plasma spraying (VPS) were almost equal [129]. A

600 °C treatment of the CoMCrSi coatings increases hardness and decreases friction against an alumina pin [130].

Abrasion resistance is better for WC-Co + CoMCrSi coatings in two-body sliding situations than for electrolytic hard chrome (EHC) coatings, but the mass loss in three-body abrasion conditions is equivalent to or even larger than that for EHC coatings [130]. A coating of WC-NiCrFeSiB is extremely resistant to oxidation and hot corrosion at temperatures as high as 800 °C [131].

For example, iron sulphide can be sprayed with HVOF liquid fuel that contains lubricants [132]. Through spraying SiO₂/Ni/Al–Si–Mg powder, resulting in MgAl₂O₄ and Mg₂Si in an AlSi matrix, for HVOF process self-propagating high-temperature synthesis (SHS) may be achieved [133]. Flight and splat stacking are the two stages of the reaction. These materials are extremely strong [134–137].

Hydroxyapatite (HAp) Coatings

For a variety of applications, including total hip and knee replacement, thermally sprayed HAp coatings enable a natural fixation on metal implants. These coatings enhance patient biomechanics, prolong the life of the implant, and improve the patient’s quality of life [138]. The only methods for creating HAp coatings that have received FDA approval are thermal plasma spray techniques [139]. However, this group of operations can result in the development of secondary phases, including amorphous calcium phosphate (ACP), tricalcium phosphate (TCP), and tetracalcium phosphate (TTCP), among others [139] since HAp is unstable at high temperatures (i.e. T > 1500 °C). The formation of these phases implies that they will be more soluble than HAp in a physiological environment, which will compromise the coating’s long-term stability [140]. The HVOF thermal spray is an alternative method to generate bioactive coatings of a quality that is equivalent to or even superior to that obtained by plasma spray [139, 141]. The HVOF enables the creation of thick, crystalline, and adherent coatings by letting the

Table 5 Comparison in between different thermal spraying techniques [78–80]

Properties	Arc spraying	Flame spraying	Plasma spraying	HVOF
Thermal source	Electric arc	Gas (O ₂ + C ₂ H ₂ , O ₂ + H ₂)	Arc of plasma	Gas (H ₂ /C ₃ H ₈ /LPG)
Particle temperature	Up to 5000 °C	Up to 3000 °C	Up to 16,000 °C	Up to 3000 °C
Particle velocity	150–300 m/s	40–150 m/s	150–600 m/s	800–1000 m/s
Max spray rate	Up to 150 kg/hr	Up to 32 kg/h	Up to 3000 kg/h	20 kg/h
Spray distance	15–25 cm	10–20 cm	14–20 cm	15–20 cm
Power input	5–10 kW	100–200 kW	Up to 200 kW	Up to 50 kW
Air flow rate	Up to 60 m ³ /h	Up to 70 m ³ /h	Up to 5.4 m ³ /h	Up to 3–4.2 m ³ /h
Type of material	Powder	Powder	Powder	Wire/powder
Bond strength	High	Excellent	Medium	Good
Hardness	High	Good	Medium	Excellent

Table 6 Comparison in between HVOF and CVD PVD process [80–94]

Factors	HVOF	PVD	CVD
Coating material	Solid form	Solid form	Gaseous form
Method	Oxygen and fuel are mixed together, fed into the combustion chamber and ignited	Atoms are transforming and depositing over the surface	Gaseous molecule will react or decompose over the substrate
Deposition temperature	Up to 3200 °C	Very low (~500 °C)	Up to 1500 °C
Cleaning requirement	High	High	Low
Noise level	High	Low	Low
Film thickness	0.1–2 mm	~3 µm	~8 µm
Film surface	Fine and dense surface without any porosity	Surface finish is very high and provide metallic lustre without grinding	Surface finish is relatively low compared to PVD
Crafting process	Generally took place at open atmosphere but in confined place as it is very noisy	Generally took place in presence of low air pressure in the reactor	Generally took place within the reactor at vacuum state
Equipment cost	Very expensive	Expensive	Cheap
Operating cost	Low to high	Moderate to high	Moderate to low
Safety	Less	High	Moderate
Adherence	Excellent mechanical bond	Moderate mechanical to good chemical bond	Good chemical to excellent diffusion bond
Coating materials	Metals, cermet, ceramics and polymers	Metals, ceramics and polymers	Metals, ceramics and polymers
Applications	Water, mining, petrochemicals, chemicals, aerospace, paper, engineering and manufacturing, gas, power, etc.	Solar panel, glass coating, aluminized PET film, snack bags, optical coatings and filters, etc.	Tool insert, semi-conductor, Aerospace industry, automobile sector, etc.

Table 7 Applications of different materials coated by HVOF technique [95–104]

Author	Coating material	Substrate	Coating thickness (µm)	Applications
Javed et al. [95]	WC-18% hastelalloy C and WC-10wt%-5wt%Cr	Monel K500	150–200	Hydraulic rig
Priyana et al. [96]	FeSiNi and FeBCr alloy powder	Grey cast iron	400	Automotive
Bansal et al. [97]	Ni ₂₀ Cr ₂ O ₃	SS202	123	Pipeline
		SS304	142	
		Mild steel	156	
Sahraoui et al. [98]	Cr ₃ C ₂ -25%NiCr WC-12%Co	AFNOR 25CD4 low-carbon steel	350	Replacement of EHC in gas turbine
Bansal et al. [99]	Cr ₃ C ₂ NiCr WC-CoCr	1Cr18Ni9Ti stainless steel	350	Hydro turbine
Vernhes et al. [100]	(a)80/20 Cr ₃ C ₂ NiCr (b) HVOF 80/20 Cr ₃ C ₂ -NiCr coating, sprayed with C3H6	Forged Inconel 718PH	215 155 ± 35	Metal-seated ball valve (steam lines in power plant)
Sidhu et al. [101]	93(WC-Cr ₃ C ₂)7Ni 75Cr ₃ C ₂ -25Ni 83WC-17W 86WC-10Co-4Cr	ASME SA213T91 steel	200–250	Boiler
Singh et al. [102]	WCO-CoCr+ MO ₂ C	SS-316	–	Pump impeller
Mahade et al. [103]	Cr ₃ C ₂ NiCr	Carbon steel	300	Automotive break disc
Gui et al. [104]	Kennametal stellite JK120H powder	N almen strip	160–180	Landing gear

powder to travel at greater speeds and lower temperatures [142]. A technique for enhancing the Osseo integration of metal implants [143]. Metal implants have a high mechanical strength, but because they are bio-inert, they have a poor ability to connect to bone tissue. Based on the favourable bioactive characteristics of several bulk ceramic materials seen in physiological conditions, bioactive coatings have been created [144]. In particular, it has been shown that the mineral HAp, $\text{Ca}_{10}(\text{PO}_4)_6(\text{OH})_2$ stimulates bone formation. Due to its chemical resemblance to the mineral component of bone, which is composed of carbonated apatite, calcium-deficient apatite, and ions such as potassium, magnesium, sodium, chloride, and fluoride, HAp has been successful as a biological material [145, 146].

Challenges and Merits of HVOF Thermal Coatings

Merits

1. As a coating material, a wide variety of substances (metal, ceramics, polymers, alloys, plastic, etc.) in different forms (powder, wire/rod) that melt without disintegrating can be used.
2. Almost any material can be coated with thermal spray paint without considerably heating the base material.
3. A thermal spray method can be used to produce the distinctive surface characteristics, such as resistance to corrosion, wear, abrasion, and dimensional restoration.
4. Compared to other processes, the thermal spray process produces less coating material waste. Therefore, when using more expensive coating materials, it is preferable to use the thermal spray procedure.
5. Effective coating can lengthen the component's lifespan.

Challenges

1. Use a line-of-sight technique.
2. During coating deposition, the material's structure and composition change.
3. The surface of the coating is uneven; therefore, some surface finishing is required to improve the surface of things.
4. Fewer process approaches for thermal spray coatings necessitating more expensive equipment result in a higher initial setup cost.
5. In certain processes (such as wire arc spray), only electrically conducting substances can be sprayed [147, 148].

Conclusions

HVOF thermal spraying is a process in which powder material is melted and propelled at high velocity towards a surface using oxygen and fuel gas mixtures. In the combustion zone, the powdered material enters the flame and becomes molten or semi-molten, depending on the melting temperature and feed rate. It is the deflagration of a C_xH_y using an oxidizing agent that is either O_2 or air at the pressure of between 0.24 and 0.82 MPa in a chamber at high velocity. Spray particle mass and temperature have a substantial influence on the critical velocities of sprayed materials and substrates, and the ideal spraying conditions have been identified based on these factors. The hitting particle will cause significant erosion if its velocity exceeds the range of hydrodynamic penetration. Compared to plasma spray coatings, wire flame-sprayed coatings have lower friction resistance but are tougher and more wear resistant. Lastly, it should be stated that a hybrid thermal spray process combining an arc spray process with an HVOF process/plasma jet process gun has been developed. In comparison with other coating processes, such as CVD, PVD and electroplating, thermal spray processes are distinguished by their high coating rates. Other advantages of thermal spray processes include the ability to deposit thick coating sections and the simplification of waste disposal. Materials sprayed with a mixture of liquid fuel and oxygen are nearly identical to those sprayed with gaseous fuel. Spraying substances containing solid fluids, such as iron sulphide, is another application for HVOF liquid fuel. In HVOF process, SHS reactions may be generated by spraying $\text{SiO}_2/\text{Nickel}/\text{Al}$ -Silicon-Mg fine particles, arising in MgAl_2O_4 , Mg_2Si in AlSi matrix, as in the case of flame or gaseous fuel. Using thermal spray methods, you can work with alloys, ceramics, polymers, cermet, and composite materials. It's also possible to create coatings with a wide range of architectural features, from thick to porous to some micrometres or millimetres dense, as well as nano- or microscale architecture.

Funding No funding has been received for this work.

Declarations

Conflict of interest The authors declare that they have no conflict of interest.

References

1. A. Raza, F. Ahmad, T.M. Badri, M.R. Raza, K. Malik, An influence of oxygen flow rate and spray distance on the porosity of HVOF coating and its effects on corrosion—a review. *Materials* (2022). <https://doi.org/10.3390/ma15186329>

2. S.K. Nayak, A. Kumar, T. Laha, Developing an economical wear and corrosion resistant Fe-Based metallic glass composite coating by plasma and HVOF spraying. *J. Therm. Spray Technol.* (2022). <https://doi.org/10.1007/s11666-021-01277-w>
3. A. Silvello, P. Cavaliere, S. Yin, R. Lupoi, I. Garcia Cano, S. Dosta, Microstructural, mechanical and wear behavior of HVOF and cold-sprayed high-entropy alloys (HEAs) coatings. *J. Therm. Spray Technol.* (2022). <https://doi.org/10.1007/s11666-021-01293-w>
4. M. Löbel, T. Lindner, T. Mehner, L.M. Rymer, S. Björklund, S. Joshi, T. Lampke, Microstructure and corrosion properties of AlCrFeCoNi high-entropy alloy coatings prepared by HVAF and HVOF. *J. Therm. Spray Technol.* (2022). <https://doi.org/10.1007/s11666-021-01255-2>
5. S.G. Sapate, N. Tansselwar, S.N. Paul, R.C. Rathod, S. Mehar, D.S. Gowtam, M. Roy, Effect of coating thickness on the slurry erosion resistance of HVOF-sprayed WC–10Co–4Cr coatings. *J. Therm. Spray Technol.* (2021). <https://doi.org/10.1007/s11666-021-01190-2>
6. S. Yan, X. Zhou, H. Zhang et al., HVOF-sprayed AlSi₅₀ alloy coatings as a novel electro thermal anti-icing/de-icing system for polymer-based composite structures. *J. Therm. Spray Technol.* (2021). <https://doi.org/10.1007/s11666-021-01243-6>
7. A. Vats, A. Kumar, A. Patnaik, M.L. Meena, Influence of deposition parameters on tribological performance of HVOF coating: a review. *IOP Conf. Ser. Mater. Sci. Eng.* (2021). <https://doi.org/10.1088/1757-899X/1017/1/012015>
8. M. Jadidi, S. Moghtadernejad, A. Dolatabadi, A comprehensive review on fluid dynamics and transport of suspension/liquid droplets and particles in high-velocity oxygen-fuel (HVOF) thermal spray. *Coatings* (2015). <https://doi.org/10.3390/coatings5040576>
9. L.M. Berger, Application of hard metals as thermal spray coatings. *Int. J. Refract. Met. Hard Mater.* (2015). <https://doi.org/10.1016/j.ijrmhm.2014.09.029>
10. G. Strafellini, M. Federici, HVOF cermet coatings to improve sliding wear resistance in engineering systems. *Coatings* (2020). <https://doi.org/10.3390/coatings10090886>
11. APS Materials, History and evolution of thermal spray coating. https://apsmaterials.com/wpcontent/uploads/2021/01/APS_Whitepaper_SM.pdf. Accessed 2 Aug 2022
12. H. Kumar, C. Chittosiya, V.N. Shukla, HVOF sprayed WC based cermet coating for mitigation of cavitation. *Eros Abrasion Hydro Turbine Bl.* (2018). <https://doi.org/10.1016/j.matpr.2017.12.253>
13. M.L. Thorpe, H.J. Richter, A pragmatic analysis and comparison of HVOF processes. *J. Therm. Spray Technol.* (1992). <https://doi.org/10.1007/bf02659017>
14. Y. Ishikawa, J. Kawakita, S. Kuroda, S. Osawa, Evaluation of corrosion and wear resistance of hard cermet coatings sprayed by using an improved HVOF process. *J. Therm. Spray Technol.* (2005). <https://doi.org/10.1361/105996305X59378>
15. N. Bala, H. Singh, J. Karthikeyan, S. Praksah, Cold spray coating process for corrosion protection: a review. *Surf. Eng.* (2014). <https://doi.org/10.1179/1743294413Y.0000000148>
16. F.L. Toma, L.M. Berger, C.C. Stahr, T. Naumann, S. Langner, Microstructures and functional properties of suspension-sprayed Al₂O₃ and TiO₂ coatings: an overview. *J. Therm. Spray Technol.* (2010). <https://doi.org/10.1007/s11666-009-9417-z>
17. C.J. Li, G.J. Yang, Relationships between feedstock structure, particle parameter, coating deposition, microstructure and properties for thermally sprayed conventional and nanostructured WC–Co. *Int. J. Refract. Met. Hard Mater.* (2013). <https://doi.org/10.1016/j.ijrmhm.2012.03.014>
18. D. Naumenko, R. Pillai, A. Chyrkin, W.J. Quadackers, Overview on recent developments of bondcoats for plasma-sprayed thermal barrier coatings. *J. Therm. Spray Technol.* (2017). <https://doi.org/10.1007/s11666-017-0649-z>
19. H. Herman, S. Sampath, R. Mccune, Thermal spray: current status and future trends. *MRS Bull.* (2000). <https://doi.org/10.1557/mrs2000.119>
20. M. Lobel, T. Lindner, T. Mehner, T. Lampke, Microstructure and wear resistance of AlCoCrFeNiTi high-entropy alloy coatings produced by HVOF. *Coatings* (2017). <https://doi.org/10.3390/coatings7090144>
21. P.L. Fauchais, J.V.R. Heberlein, M. Boulos, *Thermal Spray Fundamentals – From Powder to Part* (Springer, New York, 2014), p.1566
22. H. Katanoda, T. Matsuoka, S. Kuroda, J. Kawakita, H. Fukanuma, K. Matsuo, Aerodynamic study on supersonic flows in high-velocity oxy-fuel thermal spray process. *J. Therm. Sci.* (2005). <https://doi.org/10.1007/s11630-005-0022-2>
23. A. Dolatabadi, V. Pershin, J. Mostaghimi, New attachment for controlling gas flow in the HVOF process. *J. Therm. Sci. Technol.* (2005). <https://doi.org/10.1361/10599630522774>
24. H. Katanoda, H. Yamamoto, K. Matsuo, Numerical simulation on supersonic flow in high-velocity oxy-fuel thermal spray gun. *J. Therm. Sci.* (2006). <https://doi.org/10.1007/s11630-006-0065-z>
25. X. Yuan, H. Wang, G. Hou, B. Zha, Numerical modeling of a low temperature high velocity air fuel spraying process with injection of liquid and metal particles. *J. Therm. Spray Technol.* (2006). <https://doi.org/10.1361/105996306X124428>
26. V.R. Srivatsan, A. Dolatabadi, Simulation of particle-shock interaction in a high velocity oxygen fuel process. *J. Therm. Spray Technol.* (2006). <https://doi.org/10.1361/105996306X147126>
27. S. Gu, D.G. McCartney, C.N. Eastwick, K. Simmons, Numerical modelling of in-flight characteristics of inconel 625 particles during high-velocity oxy-fuel thermal spraying. *J. Therm. Spray Technol.* (2004). <https://doi.org/10.1361/10599630419337>
28. J. Stokes, L. Looney, HVOF system definition to maximise the thickness of formed components. *Surf. Coat. Technol.* (2001). [https://doi.org/10.1016/S0257-8972\(01\)01272-5](https://doi.org/10.1016/S0257-8972(01)01272-5)
29. S.V. Klinkov, V.F. Kosarev, Measurements of cold spray deposition efficiency. *J. Therm. Spray Technol.* (2006). <https://doi.org/10.1361/105996306X124365>
30. K. Dobler, H. Kreye, R. Schwetzke, Oxidation of stainless steel in the high velocity oxy-fuel process. *J. Therm. Spray Technol.* (2000). <https://doi.org/10.1361/105996300770349872>
31. K.V. Roa, Properties and characterisation of coatings made using Jet Kote thermal spray technique. in *Proceeding of the 11th International Thermal Spray Conference, Montreal* (1986), p. 873–882
32. F. Gartner, T. Stoltenhoff, T. Schmidt, H. Kreye, The cold spray process and its potential for industrial applications. *J. Therm. Spray Technol.* (2006). <https://doi.org/10.1361/105996306X108110>
33. D.C. Cawmer, Coating development for HVOF process using design of experiments. in *Proceedings 13th International Thermal Spray Conference, Orlando*, (1992), p. 127
34. W.J. Jarosinski, M.F. Gruninger, and C.H. Londry, Characterization of tungsten carbide cobalt powder and HVOF coatings, in: *Proceeding of the 5th National Thermal Spray Conference, California*, (1993), p. 153–158
35. T. Schmidt, F. Gärtner, H. Assadi, H. Kreye, Development of a generalized parameter window for cold spray deposition. *Acta Mater.* (2006). <https://doi.org/10.1016/j.actamat.2005.10.005>
36. T. Schmidt, F. Gartner, H. Assadi, H. Kreye, Development of a generalized parameter window for cold spray deposition. *Acta Mater.* (2006). <https://doi.org/10.1016/j.actamat.2005.10.005>
37. J. Kawakita, S. Kuroda, T. Fukushima, H. Katanoda, K. Matsuo, H. Fukanuma, Dense titanium coatings by modified HVOF

- spraying. *Surf. Coat. Technol.* (2006). <https://doi.org/10.1016/j.surfcoat.2006.01.056>
38. M. Grujicic, C.L. Zhao, W.S. DeRosset, D. Helfritsch, Adiabatic shear instability based mechanism for particles/substrate bonding in the cold-gas dynamic-spray process. *Mater. Des.* (2004). <https://doi.org/10.1016/j.matdes.2004.03.008>
 39. B.R. Marple, C. Moreau, D.V. Für-Schweisstechnik, in *Thermal Spray 2003*, ed. by C. Moreau, B. Marple (ASM International Materials Park, Ohio, 2003), pp.273–282
 40. W. Trompetter, M. Hyland, D. McGrouther, P. Munroe, A. Markwitz, Effect of substrate hardness on splat morphology in high-velocity thermal spray coatings. *J. Therm. Spray Technol.* (2006). <https://doi.org/10.1361/105996306x147261>
 41. R.G. Maev, V. Leshchynsky, Air gas dynamic spraying of powder mixtures: theory and application. *J. Therm. Spray Technol.* (2006). <https://doi.org/10.1361/105996306X108048>
 42. A.P. Alkhimov, S.V. Klinkov, V.F. Kosarev, Study of heat exchange of supersonic plane jet with obstacle at gas-dynamic spraying. *Thermophys. Aeromech.* **7**, 375–382 (2000)
 43. J. Brezinová, A. Guzanová, J. Tkacova et al., High velocity oxygen liquid-fuel (HVOLF) spraying of WC based coatings for transport industrial applications. *Metals (Basel)* (2020). <https://doi.org/10.3390/met10121675>
 44. M. Rodriguez, M. Staia, L. Gil et al., Effect of heat treatment on properties of nickel hard surface alloy deposited by HVOF. *Surf. Eng.* (2000). <https://doi.org/10.1179/026708400101517404>
 45. L.E. Gil, M.H. Staia, Effects of HVOF parameters on adhesion and microstructure of thermal sprayed NiWCrBSi coatings. *Surf. Eng.* (2002). <https://doi.org/10.1179/026708401225005377>
 46. M. Kumar, H. Singh, N. Singh, Effect of increase in nano-particle addition on mechanical and microstructural behaviour of HVOF and cold-spray Ni₂₀Cr coatings on boiler steels. *Mater. Today Proc.* (2020). <https://doi.org/10.1016/j.matpr.2020.01.321>
 47. S. Tailor, N. Vashishtha, A. Modi, Structural and mechanical properties of HVOF sprayed Cr₃C₂ 25%NiCr coating and subsequent erosion wear resistance. *Mater. Res. Exp.* (2019). <https://doi.org/10.1088/2053-1591/ab1947>
 48. V. Sreenivasulu, M. Manikandan, Hot corrosion studies of HVOF sprayed carbide and metallic powder coatings on alloy 80A at 900(C). *Mater. Res. Exp.* (2019). <https://doi.org/10.1088/2053-1591/aaf65d>
 49. Z. Cesanek, F. Houdkov-Lukac, High temperature corrosion behaviour of selected thermally sprayed coatings in corrosive aggressive environment. *Mater. Res. Exp.* (2019). <https://doi.org/10.1088/2053-1591/aae956>
 50. K. Goyal, H. Singh, R. Bhatia, Mechanical and microstructural properties of carbon nanotubes reinforced chromium oxide coated boiler steel. *World J. Eng.* (2018). <https://doi.org/10.1108/WJE-10-2017-0315>
 51. S. Vignesh, K. Shanmugam, V. Balasubramanian et al., Identifying the optimal HVOF spray parameters to attain minimum porosity and maximum hardness in iron based amorphous metallic coatings. *Def. Technol.* (2017). <https://doi.org/10.1016/j.dt.2017.03.001>
 52. S.S. Chatha, H.S. Sidhu, B.S. Sidhu, Performance of 75Cr₃C₂-25NiCr coating produced by HVOF process in a coal-fired thermal power plant. *Adv. Mater. Res.* (2016). <https://doi.org/10.4028/www.scientific.net/AMR.1137.88>
 53. B. Somasundaram, R. Kadoli, M.R. Ramesh et al., High temperature corrosion behaviour of HVOF sprayed WC–Cr–Ni coatings. *Int. J. Surf. Sci. Eng.* (2016). <https://doi.org/10.1504/IJSURFSE.2016.077542>
 54. B. Somasundaram, R. Kadoli, M.R. Ramesh, Hot corrosion behaviour of HVOF sprayed (Cr₃C₂-35% NiCr)+5% Si coatings in the presence of Na₂SO₄ 60% V₂O₅ at 700 °C. *Trans Indian Inst Met.* (2015). <https://doi.org/10.1007/s12666-014-0453-0>
 55. R. Bhatia, H.S. Sidhu, B.S. Sidhu, High temperature behaviour of Cr₃C₂-NiCr coatings in the actual coal-fired boiler environment. *Metal. Mater. Trans.* (2015). <https://doi.org/10.1007/s40553-015-0045-x>
 56. Y.Y. Santana, P.O. Renault, M. Sebastiani et al., Characterization and residual stresses of WC–Co thermally sprayed coatings. *Surf. Coat. Technol.* (2008). <https://doi.org/10.1016/j.surfcoat.2008.04.042>
 57. Y.Y. Santana, J.G. La Barbera-Sosa, M.H. Staia et al., Measurement of residual stress in thermal spray coatings by the incremental hole drilling method. *Surf. Coat. Technol.* (2006). <https://doi.org/10.1016/j.surfcoat.2006.04.056>
 58. J. Mostaghimi, S. Chandra, R. Ghafouri-Azar, A. Dolatabadi, Modelling thermal spray coating processes: a powerful tool in design and optimization. *Surf. Coat. Technol.* (2003). [https://doi.org/10.1016/S0257-8972\(02\)00686-2](https://doi.org/10.1016/S0257-8972(02)00686-2)
 59. K. Al-Athel, K. Loeffel, H. Liu, L. Anand, Modelling De cohesion of a top-coat from a thermally-growing oxide in a thermal barrier coating. *Surf. Coat. Technol.* **222**, 68–78 (2013). <https://doi.org/10.1016/j.surfcoat.2013.02.005>
 60. C.V. Di Leo, J. Luk-Cyr, L. Liu, K. Loeffel, K. Al-Athel, L. Anand, A new methodology for characterizing traction-separation relations for interfacial delamination of thermal barrier coatings. *Acta Mater.* **71**, 306–318 (2014). <https://doi.org/10.1016/j.actamat.2014.02.034>
 61. R. Ahmed, M.E. Fitzpatrick, N.H. Faisal, A comparison of neutron diffraction and hole-drilling residual strain measurements in thermally sprayed coatings. *Surf. Coat. Technol.* **206**, 4180–4185 (2012). <https://doi.org/10.1016/j.surfcoat.2012.04.018>
 62. M. Buchmann, R. Gadow, J. Tabellion, Experimental and numerical residual stress analysis of layer coated composites. *Mater. Sci. Eng. A* **288**(2), 154–159 (2000). [https://doi.org/10.1016/S0921-5093\(00\)00862-5](https://doi.org/10.1016/S0921-5093(00)00862-5)
 63. S. Kuroda, Y. Tashiro, H. Yumoto, S. Taira, H. Fukanuma, S. Tobe, Peening action and residual stresses in high-velocity oxygen fuel thermal spraying of 316L stainless steel. *J. Therm. Spray Technol.* (2001). <https://doi.org/10.1361/105996301770349457>
 64. T.C. Totemeier, R.N. Wright, W.D. Swank, Residual stresses in high-velocity oxy-fuel metallic coatings. *Metall. Mater. A* (2004). <https://doi.org/10.1007/s11661-004-0089-5>
 65. C.R.C. Lima, J. Nin, J.M. Guilemany, Evaluation of residual stresses of thermal barrier coatings with HVOF thermally sprayed bond coats using the modified layer removal method (MLRM). *Surf. Coat. Technol.* (2006). <https://doi.org/10.1016/j.surfcoat.2005.09.016>
 66. B.S. Yilbas, A.F.M. Arif, Residual stress analysis for HVOF diamalloy 1005 coating on Ti–6Al–4V alloy. *Surf. Coat. Technol.* (2007). <https://doi.org/10.1016/j.surfcoat.2007.06.049>
 67. T.S. Sidhu, S. Prakash, R.D. Agrawal, Studies on the properties of high-velocity oxy-fuel thermal spray coatings for higher temperature applications. *Mater. Sci.* (2005). <https://doi.org/10.1007/s11003-006-0047-z>
 68. J. Liu, X. Bai, T. Chen, C. Yuan, Effects of cobalt content on the microstructure, mechanical properties and cavitation erosion resistance of HVOF sprayed coatings. *Coatings* (2019). <https://doi.org/10.3390/coatings9090534>
 69. S. Thermsuk, P. Surin, Optimization parameters of WC–12Co HVOF sprayed coatings on SUS 400 stainless steel. *Procedia Manuf.* (2019). <https://doi.org/10.1016/j.promfg.2019.02.071>
 70. E. Jonda, L. Łatka, W. Pakieła, Comparison of different cermet coatings sprayed on magnesium alloy by HVOF. *Materials* (2021). <https://doi.org/10.3390/ma14071594>
 71. Y. Wang, W. Zhang, D. Chen, X. Liu, W. Hu, L. Liu, J. Yan, X. Xiong, High temperature friction and wear performance of TiB₂-50Niocomposite coating sprayed by HVOF technique.

- Surf. Coat. Technol. (2020). <https://doi.org/10.1016/j.surfcoat.2020.126766>
72. D. Mohanty, S. Kar, S. Paul, P.P. Bandyopadhyay, Carbon nanotube reinforced HVOF sprayed WC–Co coating. *Mater. Des.* (2018). <https://doi.org/10.1016/j.matdes.2018.06.054>
 73. T.K. Mishra, A. Kumar, S.K. Sinha, Experimental investigation and study of HVOF sprayed WC–12Co, WC–10Co–4Cr and Cr₃C₂–25NiCr coating on its sliding wear behaviour. *Int. J. Refract. Met. Hard Mater.* (2021). <https://doi.org/10.1016/j.ijrmhm.2020.105404>
 74. G. Digvijay, W.S. Rathod, Tribo-behaviour of APS and HVOF sprayed WC–Cr₃C₂–Ni coatings for gears. *Surf. Eng.* **37**, 80–90 (2021). <https://doi.org/10.1080/02670844.2020.1742988>
 75. S. Guha, A. Bandyopadhyay, S. Das, B.P. Swain, Synthesis and characterization of titanium silicon nitride (TiSiN) thin film: a review. *IOP Conf. Ser. Mater. Sci. Eng.* **377**, 012181 (2018). <https://doi.org/10.1088/1757-899X/377/1/012181>
 76. S. Das, S. Guha, R. Ghadai, D. Kumar, B.P. Swain, Morphological and structural properties of CVD deposited titanium aluminium nitride (TiAlN) thin films. *IOP Conf. Ser. Mater. Sci. Eng.* **377**, 012178 (2018). <https://doi.org/10.1088/1757-899X/377/1/012178>
 77. S. Guha, S. Das, Structural, morphological and mechanical property analysis of TiAlN thin film coating deposited by CVD technique, recent advances in thermofluids and manufacturing engineering. *Lect. Note Mech. Eng.* (2019). https://doi.org/10.1007/978-981-19-4388-1_36
 78. N.W. Satya, S. Mudiantoro, W. Winarto, Bond strength, hardness, and microstructure analysis of stellite coating applied on 410 steel surface using flame spray, plasma spray, and high-velocity oxy fuel spray. *IOP Conf. Ser. Mater. Sci. Eng.* (2020). <https://doi.org/10.1088/1757-899X/924/1/012016>
 79. M.H. Abd Malek et al., Thermal arc spray overview. *IOP Conf. Ser. Mater. Sci. Eng.* (2013). <https://doi.org/10.1088/1757-899X/46/1/012028>
 80. S. Guha, S. Das, A. Bandyopadhyay, B.P. Swain, Investigation of structural network and mechanical properties of titanium silicon nitride (TiSiN) thin films. *J. Alloy Compd.* (2018). <https://doi.org/10.1088/1757-899X/377/1/012181>
 81. S. Guha, S. Das, A. Bandyopadhyay, B.P. Swain, Investigation of mechanical properties of CVD grown titanium silicon nitride thin films under reduced atmosphere. *Appl. Phys. A* (2018). <https://doi.org/10.1007/s00339-017-1455-7>
 82. S. Das, S. Guha, R. Ghadai, D. Kumar, B.P. Swain, Structural and mechanical properties of CVD deposited titanium aluminium nitride (TiAlN) thin films. *Appl. Phys. A* (2017). <https://doi.org/10.1007/s00339-017-1032-0>
 83. S. Das, R. Ghadai, S. Guha, A. Sharma, B.P. Swain, Correlation of microstructural and mechanical properties of CVD deposited TiAlN coatings. *Arab. J. Sci. Eng.* (2020). <https://doi.org/10.1007/s13369-019-04202-0967-975>
 84. S. Das, S. Guha, P.P. Das, R. Ghadai, Analysis of morphological, microstructural, electrochemical and nano mechanical characteristics of TiCN coatings prepared under N₂ gas flow rate by chemical vapour deposition (CVD) process at higher temperature. *Ceram. Intern.* (2020). <https://doi.org/10.1016/j.ceramint.2020.01.023>
 85. S. Das, S. Guha, R. Ghadai, B.P. Swain, A comparative analysis over different properties of TiN, TiAlN and TiAlSiN thin film coatings grown in nitrogen gas atmosphere. *Mater. Chem. Phys.* (2021). <https://doi.org/10.1016/j.matchemphys.2020.123866>
 86. S. Das, S. Guha, R. Ghadai, A. Sharma, S. Chatterjee, Morphological, mechanical property analysis and comparative study over structural properties of CVD TiN film grown under different substrate temperature in nitrogen gas atmosphere. *SILICON* (2022). <https://doi.org/10.1007/s12633-020-00807-5>
 87. S. Das, S. Guha, R. Ghadai, A. Sharma, Influence of nitrogen gas over microstructural, vibrational and mechanical properties of CVD Titanium nitride (TiN) thin film coating. *Ceram. Intern.* (2021). <https://doi.org/10.1016/j.ceramint.2021.02.254>
 88. S. Das, D. Kumar, R. Borah, A. Dutta, S. Guha, Impact of elevated temperature over different properties of CVD SiCN coating developed in nitrogen gas atmosphere. *SILICON* (2022). <https://doi.org/10.1007/s12633-021-01631-1>
 89. S. Guha, S. Das, Investigation over effect of different carbon content on various properties of titanium carbon nitride (TiCN) coating grown on Si (100) substrate by chemical vapour deposition (CVD) process. *Eur. Phys. J. Plus* (2022). <https://doi.org/10.1140/epjp/s13360-022-02587-w>
 90. S. Guha, A. Bandyopadhyay, S. Das, B.P. Swain, Investigation of titanium silicon nitride: a review, advances in electron. *Commun. Compd Lect. Note. Electr. Eng.* (2017). https://doi.org/10.1007/978-981-10-4765-7_18
 91. S. Guha, A. Bandyopadhyay, S. Das, B.P. Swain, Synthesis and characterization of Titanium Silicon Nitride (TiSiN) thin film: a review. *IOP Conf. Ser. Mater. Sci. Eng.* (2018). <https://doi.org/10.1088/1757-899X/377/1/012181>
 92. S. Das, S. Guha, R. Ghadai, D. Kumar, B.P. Swain, Synthesis and characterization on TiAlN thin film. *Mater. Sci. Eng.* (2018). <https://doi.org/10.1088/1757-899X/377/1/012178>
 93. S. Das, M. Gupta, A. Sharma, B.P. Swain, Micro-structural and bonding structure analysis of TiAlN thin films deposited with varying N₂ flow rate via ion beam sputtering technique. *Mater. Sci.* (2022). <https://doi.org/10.2478/msp-2020-0006>
 94. S.C. Modi, E. Calla, A study of high-velocity combustion wire molybdenum coatings. *J. Therm. Spray Technol.* (2001). <https://doi.org/10.1361/105996301770349259>
 95. M.A. Javed, A.S. Mang, C.M. Bhadra, R. Neil et al., Corrosion and mechanical performance of HVOF WC-based coatings with alloyed nickel binder for use in marine hydraulic applications. *Surf. Coat. Technol.* (2021). <https://doi.org/10.1016/j.surfcoat.2021.127239>
 96. M.S. Priyana, P. Hariharana, Wear and corrosion resistance of Fe based coatings by HVOF sprayed on gray cast-iron for automotive application. *Tribol. Ind.* **36**, 394–405 (2014)
 97. A. Bansal, D.K. Goyal, P. Singh, A.K. Singla, M.K. Gupta, N. Bala et al., Erosive wear behaviour of HVOF-sprayed Ni–20Cr₂O₃ coating on pipeline materials. *Int. J. Refract. Met. Hard Mater.* (2020). <https://doi.org/10.1016/j.ijrmhm.2020.105332>
 98. T. Sahraoui, S. Guessasma, N.E. Fenineche, G. Montavon, C. Coddet, Friction and wear behaviour prediction of HVOF coatings and electroplated hard chromium using neural computation. *Mater. Lett.* (2004). <https://doi.org/10.1016/j.matlet.2003.06.010>
 99. A. Bansal, D.K. Goyal, P. Singh, A.K. Singla, M.K. Gupta, N. Bala, J. Kolte, G. Setia, Microstructure and cavitation erosion behavior of HVOF sprayed ceramic-metal composite coatings for application in hydro-turbines. *Renew. Energy* (2020). <https://doi.org/10.1016/j.renene.2020.08.099>
 100. L. Vernhes, D.A. Lee, D. Poirier, J.E. Klemberg-Sapieha, HVOF coating case study for power plant process control ball valve application. *J. Therm. Spray Technol.* (2013). <https://doi.org/10.1007/s11666-013-9978-8>
 101. V. Sidhu, K. Goyal, R. Goyal, Comparative study of corrosion behaviour of HVOF-coated boiler steel in actual boiler environment of a thermal power plant. *J. Aust. Ceram. Soc.* (2017). <https://doi.org/10.1007/s41779-017-0107>
 102. J. Singh, J.P. Singh, Performance analysis of erosion resistant Mo₂C reinforced WC–CoCr coating for pump impeller with Taguchi's method. *Ind. Lubr. Tribol.* (2022). <https://doi.org/10.1108/ILT-05-2020-0155>

103. S. Mahade, A. Mulone, S. Björklund, U. Klement, S. Joshia, Investigating load-dependent wear behavior and degradation mechanisms in $\text{Cr}_3\text{C}_2\text{-NiCr}$ coatings deposited by HVOF and HVOF. *J. Mater. Res. Technol.* (2021). <https://doi.org/10.1016/j.jmrt.2021.10.088>
104. M. Gui, R. Eybel, S. Radhakrishnan, F. Monerie-Moulin, R. Raininger, P. Taylor, Residual stress in HVOF thermally sprayed WC-10Co-4Cr coating in landing gear application. *J. Therm. Spray Technol.* (2019). <https://doi.org/10.1007/s11666-019-00894>
105. A. Edrisy, A.T. Alpas, T. Perry, Wear mechanism maps for thermal-spray steel coatings. *Metall. Mater. Trans. A* (2005). <https://doi.org/10.1007/s11661-005-0270-5>
106. T.S. Sidhu, S. Prakash, R.D. Agrawal, Characterisation of NiCr wire coatings on Ni-and Fe-based super alloys by the HVOF process. *Surf. Coat. Technol.* (2006). <https://doi.org/10.1016/j.surfcoat.2005.07.101>
107. T.S. Sidhu, S. Prakash, R.D. Agrawal, Hot corrosion resistance of high-velocity oxyfuel sprayed coatings on a nickel-base superalloy in molten salt environment. *J. Therm. Spray Technol.* (2006). <https://doi.org/10.1361/105996306x124392>
108. J. Stanisic, D. Kosikowski, P.S. Mohanty, High-speed visualization and plume characterization of the hybrid spray process. *J. Therm. Spray Technol.* (2006). <https://doi.org/10.1361/105996306x147036>
109. R. Chow, T.A. Decker, R.V. Gansert, D. Gansert, D. Lee, Properties of aluminum deposited by a HVOF process. *J. Therm. Spray Technol.* (2003). <https://doi.org/10.1361/105996303770348311>
110. T.C. Totemeier, R.N. Wright, W.D. Swank, 21st Annual Conference on Fossil Energy Materials, *Met. Mat. Trans.*51, 181e97 (2003).
111. M.E. Aalamialeagha, S.J. Harris, M. Emamighomi, Influence of the HVOF spraying process on the microstructure and corrosion behaviour of Ni-20% Cr coatings. *J. Mater. Sci.* (2003). <https://doi.org/10.1023/a:1027302122749>
112. W.J. Trompetter, A. Markwitz, M. Hyland, P. Munroe, Evidence of mechanical interlocking of NiCr particles thermally sprayed onto Al substrates. *J. Therm. Spray Technol.* **14**, 524–529 (2005). <https://doi.org/10.1361/105996305x76568>
113. Y. Kawahara, Application of high temperature corrosion-resistant materials and coatings under severe corrosive environment in waste-to-energy boilers. *J. Therm. Spray Technol.* (2007). <https://doi.org/10.1007/s11666-006-9012-5>
114. B.S. Yilbas, B.J. Abdul-Aleem, M. Khalid, Corrosion behaviour of HVOF coated sheets. *J. Therm Spray. Technol.* (2003). <https://doi.org/10.1361/105996303772082323>
115. C.R.C. Lima, J.M. Guilemany, Adhesion improvements of thermal barrier coatings with HVOF thermally sprayed bond coats. *Surf. Coat. Technol.* (2007). <https://doi.org/10.1016/j.surfcoat.2006.10.005>
116. W.R. Chen, X. Wu, B.R. Marple, D.R. Nagy, P.C. Patnaik, TGO growth behaviour in TBCs with APS and HVOF bond coats. *Surf. Coat. Technol.* (2008). <https://doi.org/10.1016/j.surfcoat.2007.09.042>
117. H. Choi, S. Lee, B. Kim, H. Jo, C. Lee, Effect of in-flight particle oxidation on the phase evolution of HVOF NiTiZrSiSn bulk amorphous coating. *J. Mater. Sci.* (2005). <https://doi.org/10.1007/s10853-005-3169-z>
118. M. Parco, L. Zhao, J. Zwick, K. Bobzin, E. Lugscheider, Investigation of HVOF spraying on magnesium alloys. *Surf. Coat. Technol.* (2006). <https://doi.org/10.1016/j.surfcoat.2006.06.047>
119. C. Deng, M. Liu, C. Wu, K. Zhou, J. Song, Impingement resistance of HVOF WC-based coatings. *J. Therm. Spray Technol.* (2007). <https://doi.org/10.1007/s11666-007-9111-y>
120. B.R. Marple, R.S. Lima, Process temperature/velocity-hardness-wear relationships for high-velocity oxyfuel sprayed nanostructured and conventional cermet coatings. *J. Therm. Spray Technol.* (2005). <https://doi.org/10.1361/10599630522729>
121. J.M. Guilemany, N. Espallargas, J. Fernandez, P.H. Suegama, A.V. Benedetti, High-velocity oxyfuel $\text{Cr}_3\text{C}_2\text{-NiCr}$ replacing hard chromium coatings. *J. Therm. Spray Technol.* (2005). <https://doi.org/10.1361/105996305x59350>
122. G.-C. Ji, C.-J. Li, Y.-Y. Wang, W.-Y. Li, Erosion performance of HVOF-sprayed $\text{Cr}_3\text{C}_2\text{-NiCr}$ coatings. *J. Therm. Spray Technol.* (2007). <https://doi.org/10.1007/s11666-007-9052-5>
123. S. Matthews, M. Hyland, B. James, Long-term carbide development in high-velocity oxygen fuel/high-velocity air fuel $\text{Cr}_3\text{C}_2\text{-NiCr}$ coatings heat treated at 900 °C. *J. Therm. Spray Technol.* (2004). <https://doi.org/10.1361/10599630421442>
124. H. Mizuno, J. Kitamura, MoB/CoCr cermet coatings by HVOF spraying against erosion by molten Al–Zn alloy. *J. Therm. Spray Technol.* (2007). <https://doi.org/10.1007/s11666-007-9046-3>
125. A.J. Horlock, Z. Sadeghian, D.G. McCartney, P.H. Shipway, High-velocity oxyfuel reactive spraying of mechanically alloyed Ni–Ti–C powders. *J. Therm. Spray Technol.* (2005). <https://doi.org/10.1361/10599630522747>
126. R.S. Lima, B.R. Marple, Optimized HVOF titania coatings. *J. Therm. Spray Technol.* (2003). <https://doi.org/10.1361/105996303770348230>
127. C.C. Stahr, S. Saaro, L.-M. Berger, J. Dubsky, K. Neufuss, M. Herrmann, Dependence of the stabilization of α -Alumina on the spray process. *J. Therm. Spray Technol.* (2007). <https://doi.org/10.1007/s11666-007-9107-7>
128. T.A. Dobbins, R. Knight, M.J. Mayo, HVOF thermal spray deposited Y_2O_3 -stabilized ZrO_2 coatings for thermal barrier applications. *J. Therm. Spray Technol.* (2003). <https://doi.org/10.1361/105996303770348320>
129. M. Ivosevic, R.A. Cairncross, R. Knight, Melting and degradation of nylon-11 particles during HVOF combustion spraying. *J Appl Polym Sci.* (2007). <https://doi.org/10.1002/app.25896>
130. M. Ivosevic, R. Knight, S.R. Kalidindi, G.R. Palmese, J.K. Sutter, Adhesive/cohesive properties of thermally sprayed functionally graded coatings for polymer matrix composites. *J. Therm. Spray Technol.* (2005). <https://doi.org/10.1361/10599630522765>
131. L. Jackson, M. Ivosevic, R. Knight, R.A. Cairncross, Sliding wear properties of HVOF thermally sprayed nylon-11 and nylon-11/ceramic composites on steel. *J. Therm Spray Technol.* (2007). <https://doi.org/10.1007/s11666-007-9088-6>
132. J. Kawakita, K. Isoyama, S. Kuroda, H. Yumoto, Effects of deformability of HVOF sprayed copper particles on the density of resultant coatings. *Surf. Coat. Technol.* (2006). <https://doi.org/10.1016/j.surfcoat.2005.02.180>
133. T.C. Totemeier, Effect of high-velocity oxygen-fuel thermal spraying on the physical and mechanical properties of type 316 stainless steel. *J. Therm. Spray Technol.* (2005). <https://doi.org/10.1361/105996305x59440>
134. G. Bolelli, L. Lusvardi, Heat treatment effects on the tribological performance of HVOF sprayed Co–Mo–Cr–Si coatings. *J. Therm. Spray Technol.* (2006). <https://doi.org/10.1361/105996306X146721>
135. T.S. Sidhu, A. Malik, S. Prakash, R.D. Agrawal, Oxidation and hot corrosion resistance of HVOF WC–NiCrFeSiB coating on Ni-and Fe-based superalloys at 800 °C. *J. Therm. Spray Technol.* (2007). <https://doi.org/10.1007/s11666-007-9106-8>
136. Y. Wang, Nano- and submicron-structured sulphide self-lubricating coatings produced by thermal spraying. *Tribol. Lett.* (2004). <https://doi.org/10.1179/174951411X12956207750544>
137. I. Ozdemir, Y. Hamanaka, M. Tsunekawa, Okumiya, in-process exothermic reaction in high-velocity oxyfuel and plasma spraying

- with SiO₂/Ni/Al–Si–Mg composite powder. *J. Therm. Spray Technol.* (2005). <https://doi.org/10.1361/105996305X59459>
138. R.G. Geesink, K. de Groot, C.P. Klein, Bonding of bone to apatite-coated implants. *J. Bone Joint Surg. Br.* (1988). <https://doi.org/10.1302/0301-620X.70B1.2828374>
139. B. Ben-Nissan, *Advances in Calcium Phosphate, Biomaterials* (Springer, Berlin Heidelberg, 2014)
140. K.D. Groot, J.G. Wolke, J.A. Jansen, Calcium phosphate coatings for medical implants. *Proc. Inst. Mech. Eng. H* (1998). <https://doi.org/10.1243/0954411981533917>
141. L. Sun, C.C. Berndt, K.A. Gross, A. Kucuk, Material fundamentals and clinical performance of plasma-sprayed hydroxyapatite coatings: a review. *J. Biomed. Mater. Res.* (2001). <https://doi.org/10.1002/jbm.1056>
142. K.A. Khor, H. Li, P. Cheang, S.Y. Boey, *In vitro* behaviour of HVOF sprayed calcium phosphate splats and coatings. *Biomaterials* (2003). [https://doi.org/10.1016/S0142-9612\(02\)00404-0](https://doi.org/10.1016/S0142-9612(02)00404-0)
143. R.A. Roşu, I. Bran, M. Popescu, C. Opreş, *In vitro* characterization of hydroxyapatite layers deposited by APS and HVOF thermal spraying methods. *Ceram. Silik.* **56**, 25–31 (2012)
144. B.G. Zhang, D.E. Myers, G.G. Wallace, M. Brandt, P.F. Choong, Bioactive coatings for orthopaedic implants—recent trends in development of implant coatings. *Int. J. Mol. Sci.* (2014). <https://doi.org/10.3390/ijms150711878>
145. H.M. Kim, Ceramic bioactivity and related biomimetic strategy. *Curr. Opin. Solid State Mater. Sci.* (2003). <https://doi.org/10.1016/j.cossms.2003.09.014>
146. M. Supova, Substituted hydroxyapatites for biomedical applications: a review. *Ceram. Int.* (2015). <https://doi.org/10.1016/j.ceramint.2015.03.316>
147. M. Prakasam, J. Locs, K. Salma-Ancane, D. Loca, A. Largeteau, L. Berzina-Cimdina, Fabrication, properties and applications of dense hydroxyapatite: a review. *J. Funct. Biomater.* (2015). <https://doi.org/10.3390/jfb6041099>
148. <https://www.irsltd.co.uk/advantages-anddisadvantages-of-thermal-spray-coatings>. Accessed 20 Oct 2022

Publisher’s Note Springer Nature remains neutral with regard to jurisdictional claims in published maps and institutional affiliations.

Springer Nature or its licensor (e.g. a society or other partner) holds exclusive rights to this article under a publishing agreement with the author(s) or other rightsholder(s); author self-archiving of the accepted manuscript version of this article is solely governed by the terms of such publishing agreement and applicable law.